PROCEEDINGS OF SPIE

Solving the MCAO partial illumination issue and laboratory results

R. Santhakumari, K. K., Arcidiacono, C., Bertram, T., Berwein, J., Herbst, T., et al.

SPIE.

Solving the MCAO Partial Illumination Issue and Laboratory Results

K. K. R. Santhakumari*[a,b], C. Arcidiacono[c,d], T. Bertram[a], J. Berwein[a], T. M. Herbst[a], R. Ragazzoni[e]

[a] Max Planck Institute for Astronomy, Königstuhl 17, 69117 Heidelberg, Germany
[b] International Max Planck Research School for Astronomy and Cosmic Physics, University of Heidelberg, Germany
[c] INAF - Osservatorio Astronomico di Bologna, Via Ranzani 1, 40127 Bologna, Italy
[d] INAF Osservatorio Astrofisico di Arcetri, Largo Enrico Fermi 5, 50125 Firenze, Italy
[e] INAF - Osservatorio Astronomico di Padova, Vicolo dell'Osservatorio 5, I - 35122 Padova, Italy

ABSTRACT

Telescopes or instruments equipped with Multi-Conjugate Adaptive Optics (MCAO) provide uniform turbulence correction over a wide Field of View (FoV), thereby overcoming the problems of isoplanatism and enabling previously challenging science. LINC-NIRVANA (LN), the German-Italian near-infrared high-resolution imager for the Large Binocular Telescope (LBT), has an advanced and unique MCAO module, which uses the Optical Co-addition of Layer-Oriented Multiple-FoV Natural Guide Star approach to MCAO with pyramid wavefront sensing. The layer-oriented wavefront correction can be performed by conjugating the Deformable Mirrors (DM) and the respective Wavefront Sensors (WFS) to the corresponding atmospheric layers. LN corrects for the aberrations in two different layers. The ground layer, conjugated to the telescope pupil ~100m above LBT, is corrected by the Ground-layer Wavefront Sensors (GWS) driving the LBT adaptive secondary mirrors, and a higher layer ~7.1km above the telescope is corrected by the High-layer Wavefront Sensors (HWS) driving a pair of Xinetics DMs on the LN bench.

At the ground layer, the footprints of the stars overlap completely and every star footprint illuminates the entire pupil-plane. However, for a higher layer, the footprints do not overlap completely and each star illuminates a different region of the conjugated plane. Lack of stars, therefore, results in some regions in this "meta-pupil"-plane not being illuminated, implying no information regarding the aberrations in these areas. The optimum way of correcting the high layer, given this limited information, is the crux of the "partial illumination issue". In this paper, we propose a solution for this issue and discuss laboratory results from the aligned LN bench in the lab. Currently, LN has completed the re-integration and re-alignment at LBT. In early June 2016, we tested our partial illumination algorithm in the instrument's final configuration in the LBT mountain lab, using simulated stars. On sky testing will begin in late 2016.

Keywords: LINC-NIRVANA, partial illumination, MCAO, adaptive optics, LBT, layer-oriented

1. INTRODUCTION

LINC-NIRVANA[1,2] (LN) is a high-resolution near-infrared imager, which will be installed on the Large Binocular Telescope[3] (LBT) in September 2016. The Multi-Conjugate Adaptive Optics[4] (MCAO) module of LN is advanced and quite unique. It takes the *optical co-addition* of *layer-oriented*[5], *multiple field of view*[6], *natural guide star* approach with *pyramid wavefront sensing*[7]. LN can provide a uniform 2' FoV correction for both "eyes" of LBT, allowing us, eventually, to do Fizeau interferometric beam combination[8]. Herbst et al.[9] explain in detail the LN optical path. The same paper also provides an overview of MCAO with LN. The complex adaptive optics system and stringent requirements due to interferometry make the alignment of the components on the LN bench and each of the sub-systems a complicated task. The details of the alignment procedures, the problems we faced, and the solutions we found to overcome them can be found in references[10-14].

---

* kalyan@mpia.de; phone: (+49) 6221 528 315; fax: (+49) 6221 528 246

LN has two pairs of wavefront sensors. A pair of Ground-layer Wavefront Sensors (GWS) conjugated to the ground-layer, ~100m above the telescope, drive the facility adaptive secondary mirrors (672 actuators) and use up to 12 stars each from an annular region 2'-6' diameter centered on the science field. Up to 8 stars from the inner 2' diameter FoV can be acquired by the two High-layer Wavefront Sensors (HWS), conjugated to 7100m above the telescope pupil. These sensors control the two commercial Xinetics deformable mirrors (349 actuators) mounted on the LN bench. This multiple FoV approach, coupled with the optical co-addition of light, allows us to use fainter stars (as long as the total flux corresponds to the limiting magnitude for the correction), thereby increasing the sky coverage. LN adaptive correction is sequential. The ground layer is corrected first by the GWS, and the HWS receives the ground-layer corrected wavefront. This makes the loop control simpler, since we may use two separate reconstruction matrices. The figure 1 explains the LN MCAO module. Note that, in order to correct the higher layer, we have to exploit the stars within the inner FoV (2' FoV in our case). Also, we define 'meta-pupil' as the projection of the 2' FoV at 7100m-conjugation altitude.
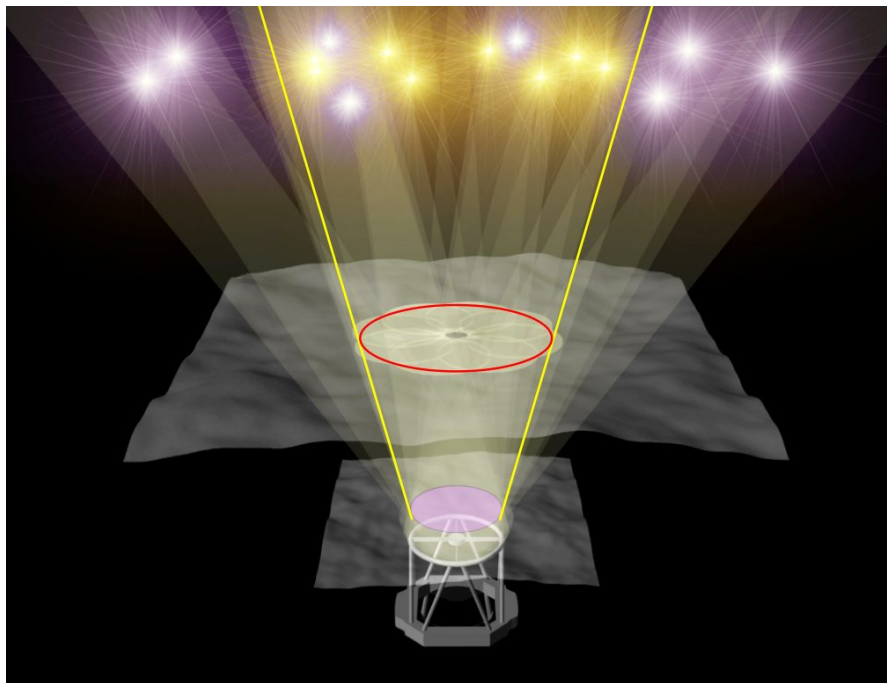

Figure 1. LN MCAO module: The ground layer and a high layer are corrected. Ground layer WFS uses information provided by the (purple) stars in the 2'-6' diameter annular FoV, while the high layer WFS uses the inner 2' diameter FoV (yellow) stars. The yellow line-segments represent the 2' FoV. The red circle represents the 'meta-pupil'.

2. DEFINING PARTIAL ILLUMINATION ISSUE

As with any MCAO system, LN faces challenges. The most important one is the 'partial illumination' issue. This is relevant for the correction of the high-layer, in our case, with the HWS. Any MCAO system that uses the layer-oriented approach will face this issue, especially if the high layer conjugated meta-pupil is larger than ~30-50% of the pupil, or in the case of very fine spatial sampling of high plane.

At the ground layer, the star footprints overlap, irrespective of the asterism. However, the footprints spatially decorrelate for higher conjugation. Inspecting the figure 1 and 2 will make this clear. The availability of the guide stars, their brightness and the asterism within the 2' FoV will vary according to where your science target is. Within the meta-pupil, there may be regions of turbulence with few overlapping stars or with only one star or even no stars. The quality of correction and the uniformity of the PSF in the entire FoV will be affected. In addition, for every new acquisition, depending on the asterism and the brightness of stars used, a different reconstruction matrix (the reconstructor of the commands to be sent to the high-conjugated DM) is necessary. This complicates the set-up of the wavefront reconstruction software. Given the limited information, how can we provide the best correction with minimum calibration time. This is the crux of the partial illumination issue[15,9].
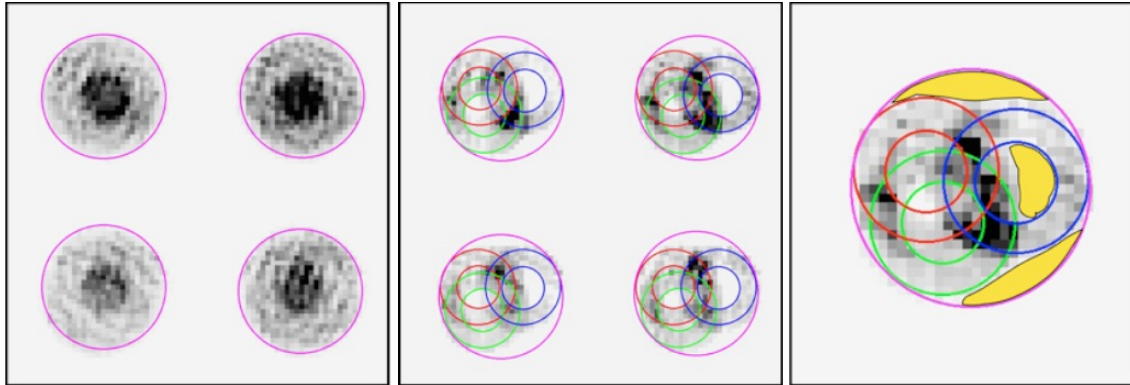
Figure 2. Real images from the HWS. The purple circle represents the meta-pupil projection on to the CCD. *left:* fully-illuminated image; *middle:* partially-illuminated metapupil image; *right:* one of the quadrants of the middle panel. The yellow shaded regions are the non-illuminated sub-apertures.

A more quantitative examination will clarify the situation. LN uses pyramid wavefront sensing. Therefore, the sub-apertures are defined at the level of the CCD (which is conjugated to the Xinetics DM). Without on-chip binning, the number of sub-apertures for a fully-illuminated metapupil is ~600 with 8 stars in a suitable asterism. However, if we are to switch off 4 of the stars (which we can do in the lab), the number of sub-apertures drops to ~400. We then have a partially-illuminated meta-pupil. We use a Signal to Noise Ratio (SNR) threshold to determine if an aperture is illuminated or not. We cannot use the same reconstruction matrix for this partial illumination case as we do for the full illumination case.

3. EXPERIMENTAL SET UP AND STRATEGY

3.1 Experimental Set Up

The experimental setup is the fully integrated and aligned LN bench, the most relevant component of which is the calibration unit. It consists of the *calibration unit folding mirror* (CU-mirror), an *absolute reference fiber* (ARF) and a *reference fiber plate* (RFP) (see figure 3). The CU-mirror is mounted in a rotating stage and it will direct the light to the HWS. The ARF defines the on-axis telescope beam. The RFP is mounted on a tip-tilt stage, which can also move along the XYZ axes. RFP has 23 fibers attached to it, defining the 'stars' in the 2' FoV. The central one is a mono-mode IR fiber, whereas all the other ones are multi-mode 200-micron fibers fed by visible wavelength LEDs. The intensities of the fibers can be remotely controlled. We can therefore imitate defined star asterisms and vary the brightness individually. The HWS has 8 probes that can move in the 2' FoV to acquire and center the stars. We can, therefore, calibrate the HWS, create partial-illumination test cases, evaluate our algorithm, and close and optimize the high-layer loop for various cases in the lab.
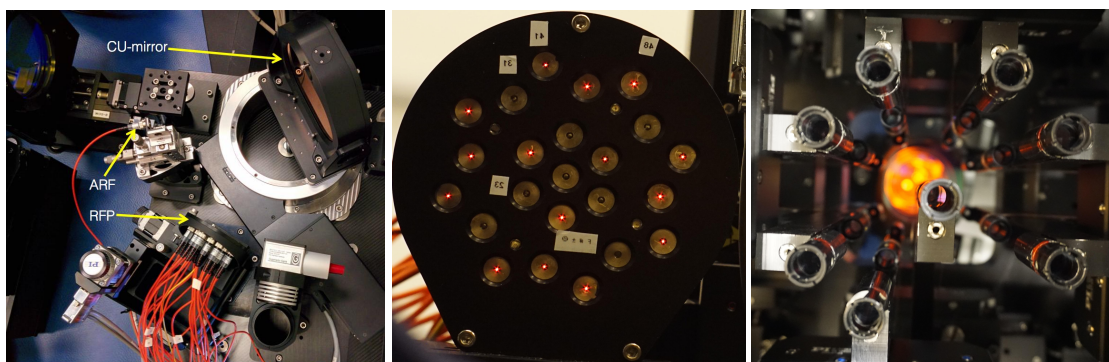

Figure 3. *left:* Calibration unit on the LN bench; *middle:* The Reference Fiber Plate (RFP). Some of the fibers are (red) illuminated; *right:* The probes in the HWS which can move in X and Y directions to acquire the stars in the 2' FoV.

3.2 Calibrating Mother Interaction Matrix

The block diagram, figure 4, explains how the injection and interaction matrices are calibrated or generated, as well as how we close the loop starting from the slope measurements to commands to the DM.
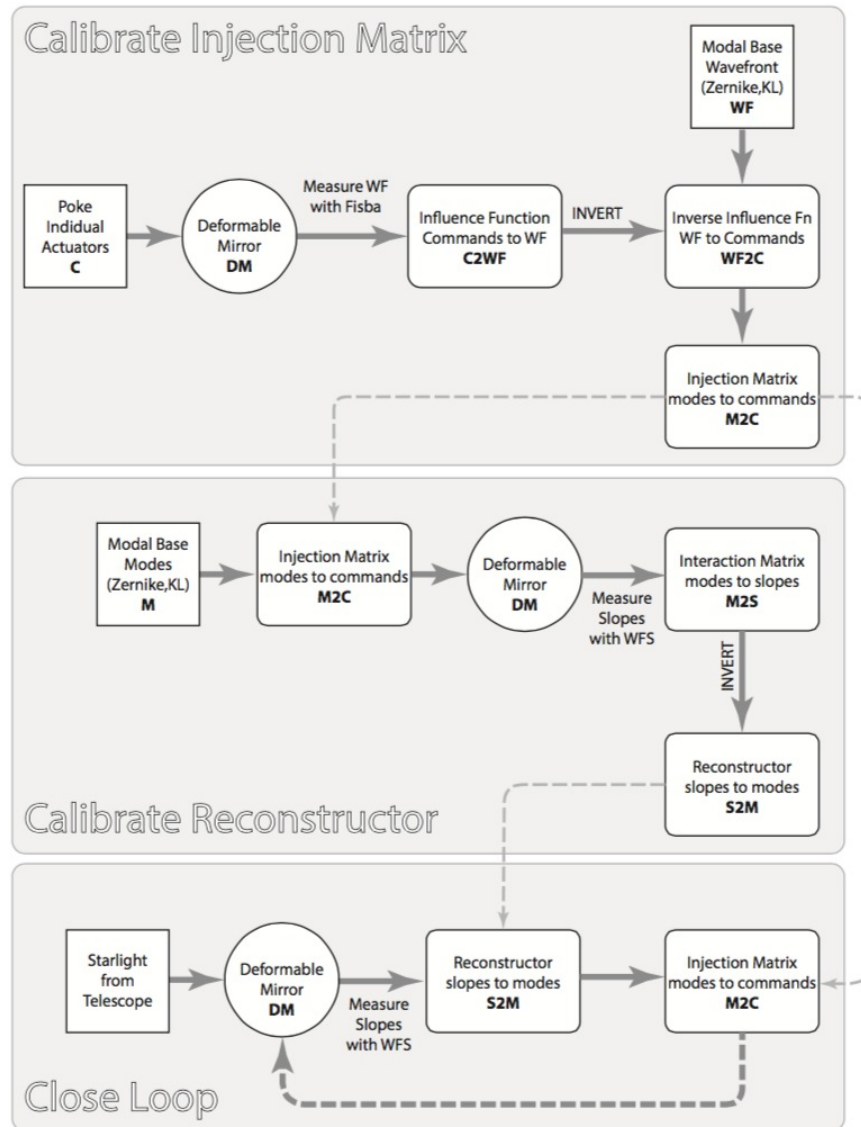

Figure 4. Step by step description of the calibration of the injection matrix and the reconstruction matrix. Also, how do we close the loop starting from the slope measurements, using the above mentioned matrices are also explained.

Our partial illumination algorithm fundamentally depends on a well-calibrated, fully-illuminated, well-conditioned interaction matrix (response of the WFS to the DM; [no. of sub-apertures X no. of modes] matrix) for the given injection matrix. We call this the 'mother interaction matrix'. By fully-illuminated, we mean that all the sub-apertures (~600) within the meta-pupil are illuminated. We can generate this in the lab using the calibration unit by illuminating the outermost fibers (numbered in the 40's), in the RFP. Prior to this, we calibrate the brightness of each of the fibers in real, on-sky magnitudes. Every fiber is illuminated by individual LEDs. Knowing the throughput of the system, quantum efficiency of the detector, the gain factor etc. we find out the fiber intensity corresponding to various magnitude stars. A SNR cut-off of 20 is used to define if a particular sub-aperture is illuminated or not. The fiber intensities are set such that all of the eight 'stars' in the 40s ring have a magnitude of 6. Once we have a fully-illuminated meta-pupil and the corresponding mask, we do the calibration to generate the interaction matrix. We run the various modes defined by the

injection matrix on the Xinetics DM and receive the slope measurements at the HWS. Analyzing the slopes, we extract the interaction matrix. Depending on the number of modes to be calibrated, the user can set the number of times this has to run so that there is sufficient SNR to get a well-conditioned matrix. Rather than running for 200 modes directly, we go in steps. First we calibrate for two modes. Here, the respective tip and tilt values are added to the DM flat values. Once we have the corresponding interaction matrix, we close the loop for the two modes and download the actuator commands (dmCommands). The average of the dmCommands, when added to the DM flat, will get us the shape of the DM corresponding to the 'pyramid flat'. Running the modes on the pyramid flat is superior to the DM flat, since this increases the pyramid sensor sensitivity and avoids WFS saturation. This is because the pyramid flat will provide the HWS with the right shape, removing the static aberrations in the optical path and other irregularities and non-uniform illumination due to dust etc. We then do the calibration for 5 modes on the pyramid flat. We follow the same procedure for calibrating a higher number of modes. Each time, the latest pyramid flat for the highest number of modes previously calibrated is used. Also, the number of iterations is increased as we calibrate a higher number of modes. Finally, we get the well-conditioned mother interaction matrix (condition number of ~25 for ~200 modes). We have developed a python code, which can communicate with the instrument and perform all of the above in a fully automatic way. We do not have to do the calibration on sky: all this can be done during the day using the calibration unit.

3.3 Extracting the Daughter Interaction Matrix for the Respective Partial Illumination Cases

There will always be fewer and fainter reference stars than desired, and thus, we are certain that almost every time we will have partial illumination. Therefore, we will have a different mask for every asterism and brightness distribution. It is essential to have the correct interaction matrix matching the sub-apertures to close the loop. Calibrating a new interaction matrix for each asterism would consume a lot of observing time. To avoid this, we came up with the following algorithm. We extract the 'daughter interaction matrix' for the respective partial illumination mask from the mother interaction matrix that we already calibrated. By doing so, we do not have to calibrate every time, but only to get the mask for the present star configuration.

This works as follows: Illuminated sub-apertures within any of the partial illumination cases will be a subset of the fully-illuminated case. The mother interaction matrix has the information regarding every sub-aperture for every calibrated mode. From the mother interaction matrix, we remove those columns corresponding to the non-illuminated sub-apertures of the partial illumination case under consideration to get the daughter interaction matrix. Inverting the daughter interaction matrix produces the reconstructor for the partial illumination case. This takes less than one minute (the acquisition and centering time not included). This reconstruction matrix is registered to close the loop for the respective mask. We have developed a python code that can perform this.

4. RESULTS & DISCUSSION

The code also allows us to test various configurations of the partial illumination case. We recently achieved lab confirmation that our algorithm works fine. This section reports on the most important observations.

4.1 Injection Matrix

The first set of partial illumination data was obtained during July 2015, when LN was at MPIA, a few weeks before dis-assembly for packing and shipping to LBT. At that time, we used a Zernike modal basis injection matrix. There were many complications and we could not always stabilize the closed loop in the partial illumination case. Analyzing the data later on, we found a few bugs in the code. Also, the injection matrix we used had a few actuators with zero values. Irrespective of these faults, it was clear that a Zernike modal basis produced higher dmCommands values at the edge of the meta-pupil, even for the full illumination case. Though stable partial illumination correction was not possible, we could correct up to 200 modes for full illumination.

Recently, we got our next set of data from the re-aligned LN bench in the mountain cleanroom of LBT. We started again with the injection matrix based on a Zernike modal basis. We followed the same steps for calibration, mask creation and partial illumination. We observed the same trend of higher actuator values at the edge of meta-pupil. Therefore, we moved to a Karhunen–Loève (KL) basis. The KL basis was created knowing the projection of the meta-pupil on the DM and an assumed Kolmogorov power spectrum of atmospheric turbulence. A few actuators at the edges of the DM did not have proper influence function measurements, due to the geometry of the optics on the LN bench causing vignetting on the DM mount. These actuators were slaved to the nearest actuators in the radial direction. Using the actuator influence functions and the response of poking each actuator on the HWS, we generated the injection matrix. However, this resulted in higher values for the edge actuators and therefore produced instability in closed loop. We therefore made a synthetic KL basis injection matrix, using only the projection of the meta-pupil on the DM. The synthetic injection matrix produced reasonable actuator values at the edge of the meta-pupil, as well as for the outermost actuators. The

closed-loop was considerably more stable. As a result, we chose to use the synthetic KL basis injection matrix[9] (>200 modes) for calibration and for partial illumination.

4.2 CCD Displacement

It is very important that the position of the CCD remain the same throughout this process. A couple of times, when the computer running the CCD services crashed, we had to re-initialize the CCD position. After this procedure, we had a displacement of up to 2 pixels in one direction. The effect was very evident while closing the loop. The actuators became unstable after a few frames and loop opened. This was because of the mis-alignment (or mis-registration) between the sub-apertures and the actuators in the new configuration. Therefore, every time we cross check the CCD position by minimizing the mean square difference between the full illumination mask and a theoretical one. The team is currently refining the CCD positioning service to ensure that the CCD is always in the correct position, even when the instrument is tilted (e.g. when telescope is at horizon).

4.3 Partial Illumination Algorithm Tested Positive

We have tested our partial illumination algorithm and the code. It is working. Combinations with 3 to 8 stars in different asterisms were considered. The brightness of the stars was also varied. However, for this run, we chose to stay in the brighter side, from 5mag till 9mag. Each time, we used a utility called 'automatic gain control'[9] to automatically get the best gain values for the configuration. Typically we assign one gain to tip and tilt, a second one to modes from 3 to 50 and a third gain to the higher modes. An initial reasonable guess has to be provided. The RMS value of the residual wavefront slopes is used as the merit function. The converged value, while the loop is stable, is used to close the loop for the given case. In the code, there is provision for setting a different mother interaction matrix with less or more number of modes, if necessary.

Our general conclusions are the following. (1) More illuminated sub-apertures means better correction (or lower RMS wavefront error). Also, more modes can be corrected in this instance. (2) It is better to have more or less equal brightness stars (providing more or less uniform SNR). Obviously the brighter they are, the better. However, the instabilities start appearing for lower number of modes if there is one star that is really bright (say 5mag) and others fainter (say, one 8mag and one 7mag). (3) We did try for 1-star and 2-star combinations. However, the loop is currently unstable in this situation. We believe that this instability arises because the modal basis is no longer orthogonal for these small scales. Note that the modal basis is defined over the entire meta-pupil. (4) For 3 star asterisms, we could close the loop for more than 100 modes. We were able to close the loop using ~200 modes for 4 star asterisms and higher.
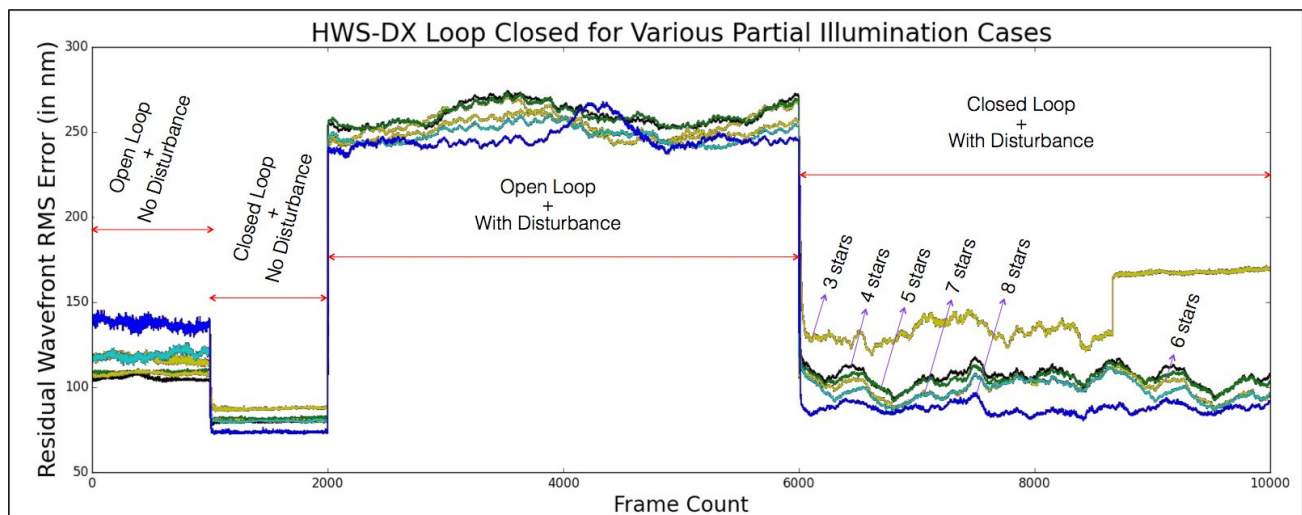

Figure 5. Residual wavefront RMS error plotted against frame for various partial illumination cases tested in the lab. Frames 0-999 correspond to open loop (showing the static aberrations seen by the HWS), frames 1000-1999 correspond to the close loop (the static aberrations are removed by the HWS), frames 2000-5999 correspond to open loop with a disturbance (aberrations send directly to the DM) running, frames 6000-10000 correspond to the loop being closed while the disturbance is also send to the DM. Different colors, marked accordingly, represent various partial illumination cases from 3 to 8 star combinations. It is evident that the correction is better as you go from 3 to 8 star combinations, since more sub-apertures are illuminated. For the cases plotted above, we have used more or less similar bright magnitude stars (fibers in the RFP), except for the 3-star combination where we have taken 5mag, 8mag, and 10mag stars. Large difference in brightness caused instabilities in the loop. The actuators corresponding to the non-illuminated sub-apertures received bogus values from the HWS. The loop got open around frame 8800, and the DM does not move any more.

At this writing (mid June 2016), it is only a week after getting the data. The analysis will obviously continue. Also, we will be acquiring more data, this time with fainter stars as well, remotely working from MPIA. On-sky testing will begin toward the end of this year.

REFERENCES

[1] T. M. Herbst et.al, "The LINC-NIRVANA Fizeau interferometric imager: final lab integration, first light experiments and challenges," Proc. SPIE 9146, Optical and Infrared Interferometry IV, 91460I (24 July 2014); doi: 10.1117/12.2055495.

[2] T. M. Herbst et.al, "LINC NIRVANA at LBT: Final Preparations for First Light," This conference (SPIE 2016).

[3] J. M. Hill et.al, "The Large Binocular Telescope," Proc. SPIE 8444, 844445 (2012).

[4] J. M. Beckers, "Detailed Compensation Of Atmospheric Seeing Using Multiconjugate Adaptive Optics," Proc. SPIE 1114, Active Telescope Systems, 215 (September 20, 1989); doi: 10.1117/12.960826.

[5] R. Ragazzoni et.al, "Adaptive optics for 100-m-class telescopes: new challenges require new solutions," Proc. SPIE 4007, Adaptive Optical Systems Technology, 1076 (July 7, 2000); doi: 10.1117/12.390313.

[6] R. Ragazzoni et.al, "Multiple field of view layer-oriented adaptive optics. Nearly whole sky coverage on 8m class telescopes and beyond," A&A 396, 731–744 (2002).

[7] R. Ragazzoni, "Pupil plane wavefront sensing with an oscillating prism," Journal of Modern Optics 43, 289–293(Feb.1996).

[8] P. Bizenberger et al., " LINC-NIRVANA: optical design of an interferometric imaging camera," Proc. SPIE 6269, 62690D (2006).

[9] T. M. Herbst et al., "MCAO with LINC-NIRVANA at LBT: Preparing for First Light," This conference (SPIE 2016).

[10] L. Marafatto et al., "Aligning more than 100 degrees of freedom wavefront sensor," Proc. SPIE 8447, 84476F-1 (2012).

[11] K. K. R. Santhakumari et.al, "Ground layer correction: the heart of LINC-NIRVANA," Proc. SPIE 9148,914897 (2014).

[12] L. Marafatto et al., "Aligning the LINC-NIRVANA natural guide stars MCAO system," AO4ELT4 conference proceeding, October 2015.

[13] J. Moreno-Ventas et.al, "Optical integration and verification of LINC-NIRVANA," Proc. SPIE 9147, Ground-based and Airborne Instrumentation for Astronomy V, 91473V (8 July 2014); doi: 10.1117/12.2057456.

[14] J. Moreno-Ventas et.al, "Final integration and alignment of LINC-NIRVANA," This conference (SPIE 2016).

[15] T. Bertram et.al, "Wavefront sensing in a partially illuminated, rotating pupil, "Proc. SPIE 9148, Adaptive Optics Systems IV, 91485M (22 August 2014); doi: 10.1117/12.2057384.